CDF/ANAL/JET/CDFR/10228
Draft 0.1
July 5, 2012

Exclusive Central Meson Production in Proton Antiproton Collisions at the Tevatron

Artur Swiech, Maria Zurek
Jagiellonian University, Cracow, Poland

Michael Albrow, Jonathan Lewis
Fermi National Accelerator Laboratory, USA

Denys Lontkowsky, Inna Makarenko
Univ. of Kiev, Ukraine

Abstract

It has been known since the days of the Intersecting Storage Rings, ISR, at CERN, that one can have pp interaction with more than one pomeron, $\mathbb{P}$, exchanged, known as double pomeron exchange. Exclusive hadronic systems, produced by double pomeron exchange, D$\mathbb{P}$E, have the potential of opening a rich new window on hadron spectroscopy and diffraction mechanism.

We have studied events of the type $p + \bar{p} \to p + X + \bar{p}$ where X is a hadron pair (mostly $\pi^+\pi^-$) at $\sqrt{s}$ = 900 GeV and 1960 GeV in the Collider Detector at Fermilab (CDF). The hadron pair is central, $y \approx 0$, and between two rapidity gaps $\Delta y \approx 4$. The dominant process is double pomeron exchange, D$\mathbb{P}$E, with restrictions on the quantum numbers of X: Q = S = 0, C = +1, J = 0 or 2. The mass spectra, with about 300K candidate events assumed to be $\pi^+\pi^-$, shows strong resonant structures attributed to f_0 and f_2 states. We give the ratio of cross sections at $\sqrt{s}$ = 900 GeV and 1960 GeV, and compare with Regge expectations.

1 Introduction

The pomeron, $\mathbb{P}$, can be defined as the carrier of 4-momentum between protons when they scatter elastically at high (i.e. collider) energies. It is therefore a strongly interacting color singlet state, at leading order a pair of gluons: $\mathbb{P}$= gg. Of course in QCD it cannot be a pure state, quark pairs and other gluons must evolve in when Q^2, which we can equate with the 4-momentum transfer[2] t, becomes large. When Q^2 is small ($\lesssim$ 2 GeV^2) which is usually the case with pomeron exchange, perturbative QCD cannot be used to calculate cross sections, as the coupling $\alpha_s(Q^2)$ becomes of order 1. Non-perturbative methods, such as Regge theory, are more applicable [1, 2, 3]. It is a challenge to theorists to derive Regge theory from QCD, but after 40 years it has not happened. Meanwhile the subject is largely data-driven and phenomenological, hence the value of new data such as in this study.

It has been known since the days of the Intersecting Storage Rings, ISR, at CERN (pp with $\sqrt{s} = 23 - 63$ GeV) that one can have pp interactions with more than one pomeron, $\mathbb{P}$, exchanged, known as double pomeron exchange, D$\mathbb{P}$E. See [4] for a recent review. This process $\mathbb{P}$+$\mathbb{P}\rightarrow X$ allows an experimental approach to better understand the pomeron. One should not think of the pomerons as isolated entities being emitted from the protons that then interact; the pomeron is only a t-channel exchange. D$\mathbb{P}$E can also be thought of as $g + g \rightarrow X$ with another (soft) gluon(s) exchanged to cancel the color and allow the protons to (sometimes) emerge intact. Sometimes the protons will dissociate into a low-mass state, e.g. $p \rightarrow p\pi^+\pi^-$. This is diffractive dissociation; it should not affect the properties of X. In CDF we cannot detect the outgoing protons, but it does not matter for this study as long as we can select events with large rapidity gaps $\Delta y \gtrsim 3$ on each side of X.

When $M(X) \lesssim 4$ GeV/c^2 the interest is for specific ("exclusive") states with well defined quantum numbers; when $M(X) \gtrsim 10$ GeV/c^2 the (multi-)partonic structure of the pomeron is probed, and one may find new phenomena related to the fact that it is *not* a hadron, but is nevertheless a strongly-interacting color singlet without valence quarks. High mass central states the subject of a different study.

Understanding these interactions will enhance our understanding of non-perturbative QCD. CDF is an excellent detector for this physics, and while the LHC detectors would be suitable, the running conditions are now such that there are very few interactions with no pile-up, which is a necessary condition for this physics (unless one measures both leading protons, as in the FP420 projects). However at least CMS and ALICE are studying these low mass exclusive hadron processes (there are no publications as yet).

2 Relevant CDF detectors

For the results in this study we used all the CDF detectors with the exception of the time-of-flight system. The muon chambers are used only for background rejection, and silicon dectector for track quality enchancment. We will select events with just 2 or 4 COT tracks, with $\sum Q = 0$. We want to select events with no other hadrons produced, and will require that all the calorimetry (except around the impact points of the charged particles), the BSC-1 counters, and the CLC have signals consistent with noise. This data was taken after the outer BSC counters (BSC-2 and BSC-3) and the MiniPlug were decommissioned. We are therefore blind to $|\eta| > 5.9$ and accept events where the proton was quasi-elastically scattered ("el") or where it fragmented into a low mass state ("inel"). There will be three classes: el+el, el+inel, and inel+inel.

3 Rapidity gap cuts, exclusive selection

In this section we explain the off-line selection of exclusive 2-track (h^+h^-) and 4-track ($h^+h^-h^+h^-$) events. To understand the noise levels in all the detectors, we use zero-bias (bunch crossing) triggers, taken during the same periods. We did this independently for the 1960 GeV and 900 GeV runs. We divided the 0-bias data into two classes: (A) No interactions, defined as no tracks, no muon stubs and no CLC hits, (B) all the other events, totally dominated by one or more inelastic interactions. For each subdetector we compare the signals in the two classes, with (A) dominated by noise. We (in CDF) have previously successfully used this method in two ways. In the search for exclusive Z-boson and observation of high mass lepton pairs [7], we summed the signals (e.g. ADC counts) in each subdetector, and imposed cuts on the sums. In our observations of exclusive χ_c [6] and $\gamma\gamma$ [8] we did not sum, but plotted the hottest channel, e.g. the PMT with the highest signal, and required that to be less than a cut. The methods give similar results.

3.1 Forward gaps

To illustrate the forward gaps selection with the detectors in the trigger, Fig. 1 shows the distribution of the sum of the BSC-1 West ADC counts (4 PMTs) ($\log_{10}$ scale) showing the noise-dominated and signal-dominated distributions. The interaction data shows a component at the noise level, because of course a sizeable fraction of interaction events have a gap in this counter, which only covers 0.5 units of pseudorapidity. Fig. 2 presents similar interaction - no interaction separation in Forward Electromagnetic West Plug detector determined for Zero-Bias data taken from same period as triggered data. These are for the west side detectors; the plots on the east side are very similar, for all the sub-detectors, and the same cuts were made on both sides. The analogous procedure was done for CLC and Forward Hadronic Plug detector.

3.2 Central region exclusivity

We now require that the central detectors are clean, except for the two (or four) charged tracks. The tracks are extrapolated to the calorimeters, and allowing any energy in a cone $\sqrt{\eta^2+\phi^2} < 0.3$ around the impact points we apply the same procedure as in the forward detectors. Fig. 3 shows the ($\log_{10}$) energy distribution in the central calorimeters.

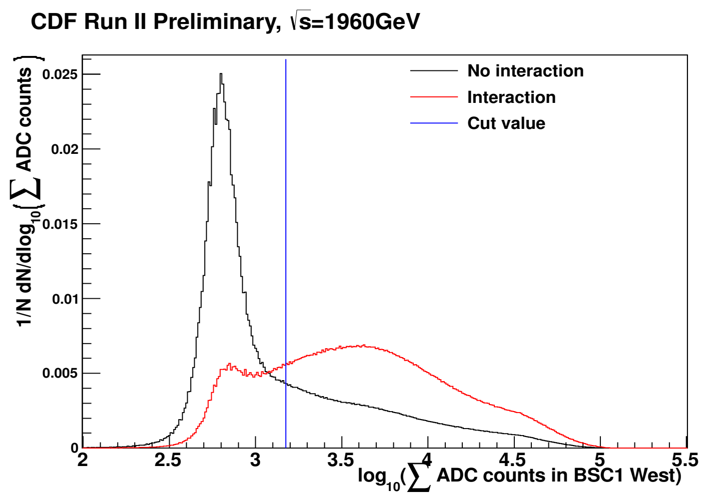

Figure 1: Interaction - No interaction separation in Bsc1 West detector determined for Zero-Bias data taken from same period as triggered data.

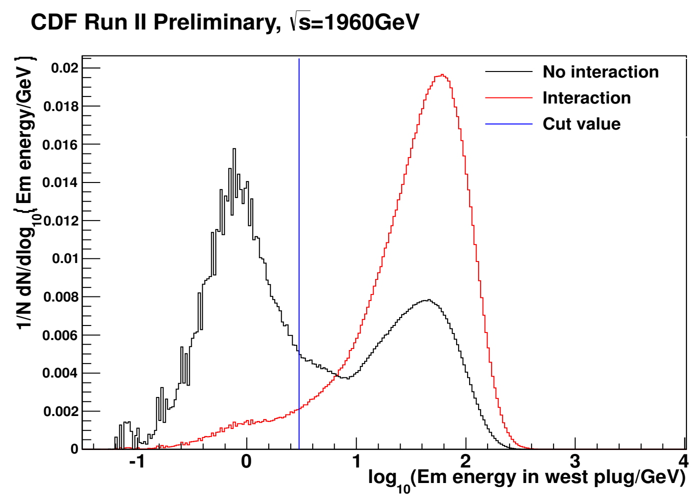

Figure 2: Interaction - No interaction separation in Forward Electromagnetic West Plug detector determined for Zero-Bias data taken from same period as triggered data.

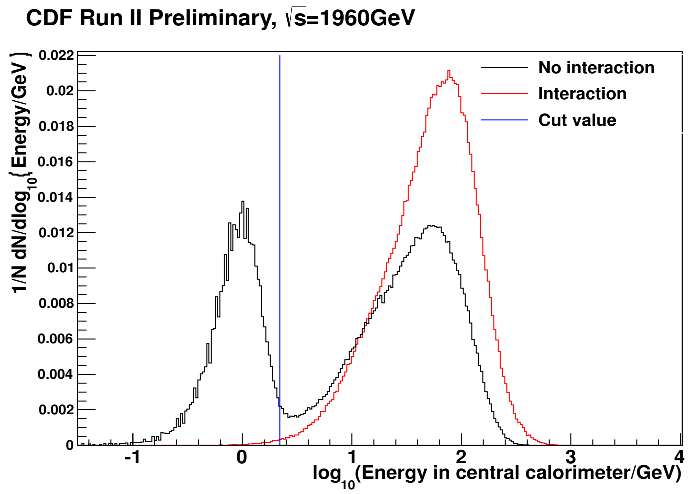

Figure 3: Interaction - No interaction separation in Central Calorimeter detector determined for Zero-Bias data taken from same period as triggered data. $\sqrt{s} = 1960$ GeV.

4 Exclusive efficiency and effective luminosity

As any cross sections that we measure uses data with no other inelastic collision to spoil the exclusivity (no pile-up), we need to know the probability of having no pile-up. This is the *exclusive efficiency* $\varepsilon(excl)$. As in our previous publications, the method is to look at 0-bias data, for which the luminosity of the particular bunch crossing, L_{bunch}, is recorded. Applying all the same cuts as before, we measure, as a function of L_{bunch}, the probability $P(0)$ that all the detectors are in the noise, so apparently there was no inelastic collision (except low mass diffraction with very forward fragmentation products). The average number of such inelastic collisions is $\bar{n} = \mu = L_{bunch} \times \sigma_{inel-vis}/f_X$, where f_X is the orbital frequency of the Tevatron (i.e. the number of times per second a particular bunch passes, which is 186,000 m/s $\div$ 4 m = 46,500/s). (m = miles.) As the actual number follows a Poisson distribution, $P(0) = e^{-\mu}$. This is plotted in Fig. 4 with an exponential fit. The fit should extrapolate to 1.0 at $L_{bunch} = 0$, and it is very close, meaning that there is almost no noise above the cuts that would give a non-empty detector even with no luminosity. The slope (if the bunch luminosity is known) in principle gives $\sigma_{inel-vis}$, or rather the cross section for producing any hadrons in $-5.9 < \eta < +5.9$, which does not include low mass diffraction. Note that the beam (true) rapidity is $y = ln(\sqrt{s}/m(p)) = 7.64$. Although true rapidity and pseudorapidity are not the same, especially very forward, a "rule of thumb" allows diffractive masses up to about 20 GeV/c^2 to escape in the forward region.

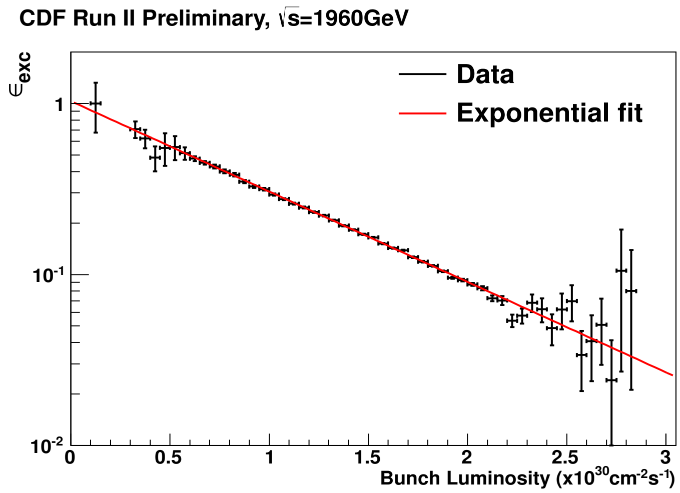

Figure 4: Exclusive efficiency as a function of bunch luminosity for $\sqrt{s} = 1960$ GeV.

5 Two exclusive tracks; track quality cuts

The selection of 2-track events is made with a sequence of cuts. We give higher priority to having a clean, well measured, sample than to efficiency. A big reduction comes from the central exclusivity requirement. A large part of that probably comes from expected events with two charged tracks + neutrals (especially π^0).

We use the higher statistics 1960 GeV data to define the track cuts, and apply the same cuts at 900 GeV. The cut at $|\eta| = 2.1$ is only to have a well defined boundary. The opening angle cut, removes a small number of cosmic ray tracks with $\theta_{3D} \approx \pi$. Both tracks are required to have an impact parameter to the nominal beam line less than 0.5 mm, and to have a difference in z projected to the beam line $|dz_0| < 1.0$ cm. The impact parameter distributions are shown in Fig. 5. The position of these cuts is chosen (rather subjectively) to eliminate events that are not as well measured.

We require both tracks to have > 25 axial hits and > 25 stereo hits, and $\chi^2/\text{ndof} <$ 2.5 to have good quality tracks. To have a well-defined fiducial region and avoid poorly known thresholds we require both tracks to have $P_t > 0.3$ GeV/c. The $P_t(pair)$ (the 2-vector sum) was required to be $P_t(pair) < 2.0$ GeV, see Fig.6. This does not reject many events, and a very small fraction of real $D\mathbb{P}E$ events would have such high P_t (the protons roughly follow a distribution $e^{-7|t|}$) so the background may be higher in these events. Finally we require the tracks to have opposite charge. The numbers of (++) and (- -) pairs are similar.

We are left with 299,931 events at 1960 GeV and 11,164 at 900 GeV.

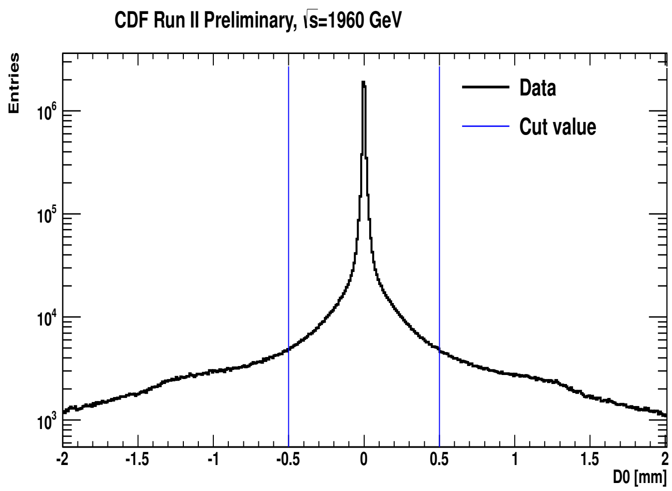

Figure 5: Impact parameter distribution with cut shown as a blue line.

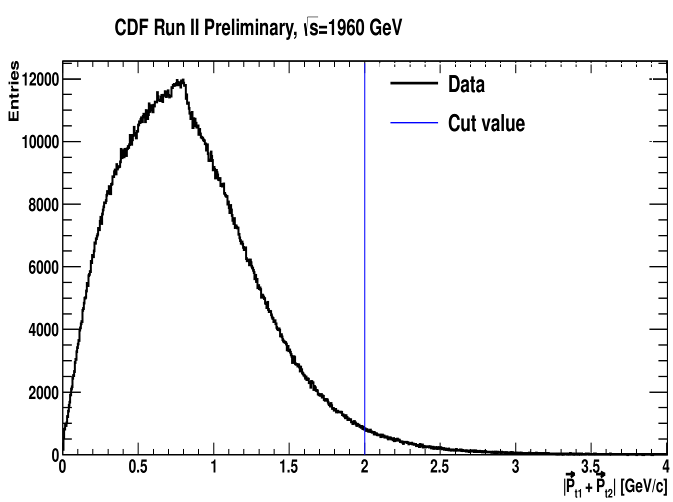

Figure 6: Distribution of track P_t with cut shown as a blue line.

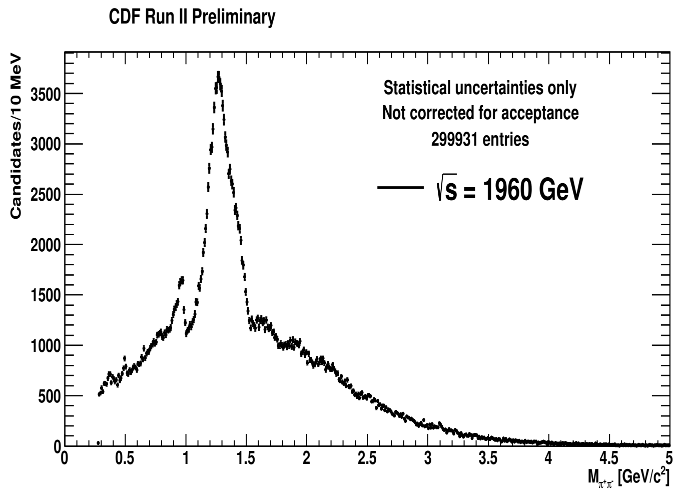

Figure 7: Invariant mass distribution of 2 particles assuming pion mass - not corrected for acceptance. $\sqrt{s} = 1960$ GeV

5.1 Mass distributions, resonance structures, and kinematic properties

We now present mass spectra uncorrected for acceptance, after which we will discuss the Monte Carlo calculations of acceptance and correct to give the cross sections. As the trigger required two towers with $E_T > 0.5$ GeV, a state with $M(X) \lesssim 1$ GeV will not be accepted if it has very small P_t. So the acceptance is a strong function of both $P_t(X)$ and $M(X)$ when these are both small.

Table 1 shows all the states with allowed quantum numbers $I^G J^{PC} = 0^+(0/2)^{++}$ up to 1500 MeV. There are some higher broad states, mostly not well established. This data may make a valuable contribution to meson spectroscopy. States with a large gluonic content ("glueballs" or hybrids) should be favored, in contrast to $\gamma\gamma \to X$ where $q\bar{q}$ stated are favored.

Fig. 7 and Fig. 8 show the mass distributions of the events in 10 MeV/c^2 bins, for all P_t, with statistical errors only. We have not used any particle identification, and assume here that h^+h^- is $\pi^+\pi^-$. This was found to be a good approximation in D$\mathbb{P}$E at the CERN ISR.

Fig. 9 shows, on a log scale, the ratio of data (1960/900).

While the ratio is consistent with being constant from threshold up to 1 GeV/c^2, it drops significantly in the mass region of the $f_2(1270)$. The lower ratio there is perhaps a spin effect. The downward trend of the ratio continues to above 4 GeV/c^2. The overall behavior of the $\sqrt{s}$ dependence as a function of mass gives a good benchmark to test models.

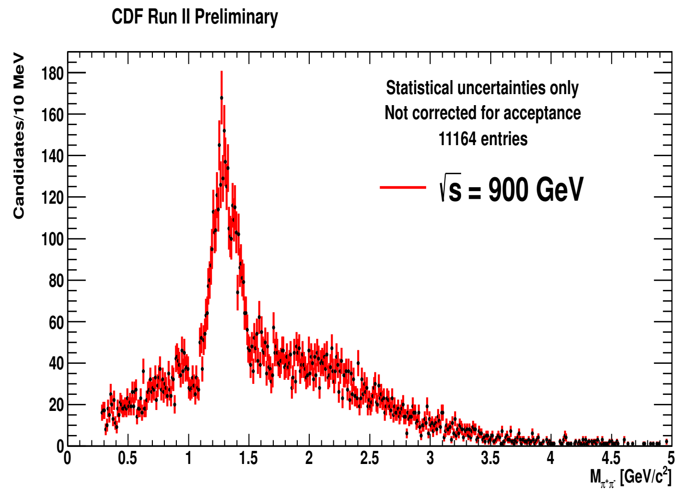

Figure 8: Invariant mass distribution of 2 particles assuming pion mass - not corrected for acceptance. $\sqrt{s} = 900$ GeV

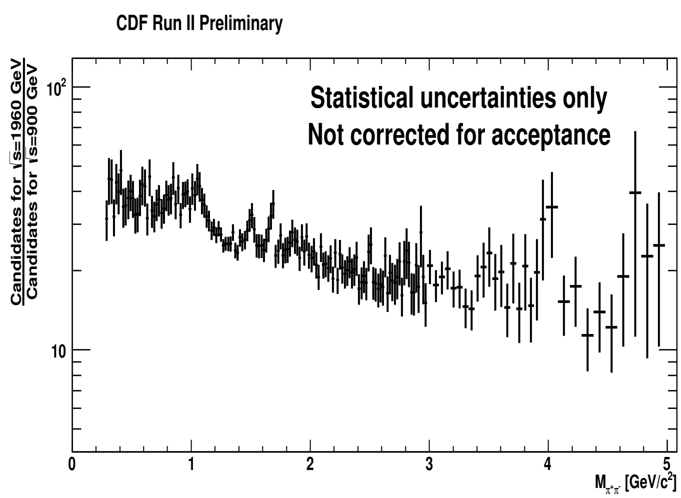

Figure 9: Ratio of mass distributions for $\sqrt{s} = 1960$ GeV and $\sqrt{s} = 900$ GeV

Name	Mass(MeV/c^2)	Width (MeV/c^2)	B.R. $\pi^+\pi^-$
$f_0(600)$ or σ	400-1200	250-500	$\sim 100\%$
$f_0(980)$	980$\pm$10	40-100	$\sim 100\%$
$f_2(1270)$	1275.1$\pm$1.2	$185.1^{+2.9}_{-2.4}$	$56.5^{+1.6}_{-0.8}\%$
$f_0(1370)$	1200-1500	150-250	seen
$f_2(1430)$	$\sim$ 1430	?	seen
$f_0(1500)$	1505$\pm$6	109$\pm$7	23.3$\pm$1.5%
$f_2'(1525)$	1525$\pm$5	73$\pm$6	0.5$\pm$0.1%

Table 1: Mesons in PDG allowed in DIPE. Higher mass states can be added.

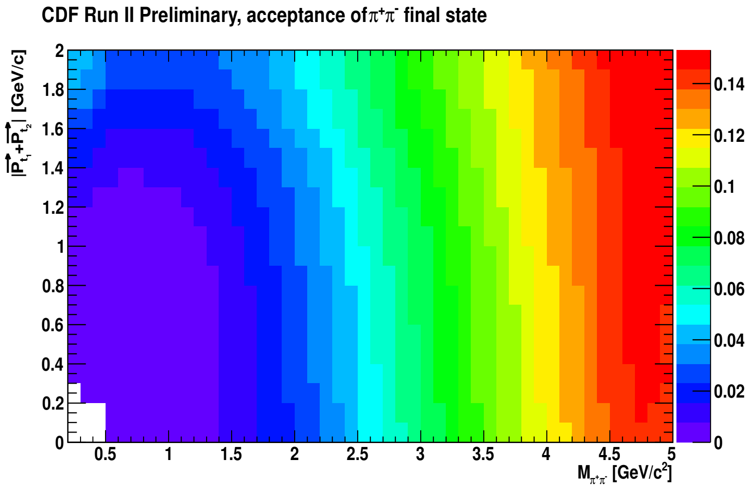

Figure 10: Acceptance as a function of invariant mass and P_t of central state, assuming isotropic (J=0, S-wave) decay to 2 charged pions.

6 Acceptance calculation

In order to present cross sections, such as $d\sigma/(dM.dP_t.dy)$ and unfold acceptance $A(M, P_t, y)$ from the data, we calculate the acceptance, generating pion pairs and using CDFSIM to simulate the trigger and resonstruction efficiency. A parent state X is generated, flat in rapidity with $-2.1 < |y| < +2.1$, flat in mass $M(X)$ from 0 to 5.0 GeV/c^2, and flat in P_t from 0 to 2.5 GeV/c. In the absence of knowledge about spins and polarizations, X is made to decay isotropically (S-wave, J=0), and the final state particles are then specified, and one tests the simulated trigger, etc.

In the acceptance calculation the showers made by the pions in the calorimeter were simulated and the 2CJET0.5 trigger requirement checked. At least two towers with $E_T > 0.5$ GeV were required. The forward off-line cuts were made (a decay particle could be forward, even if X was more central). The additional track cuts were simulated, and the acceptance $A(M, P_t)$ calculated as the ratio of generated to accepted events in bins of $M(X)$ and $P_t(X)$. Finally, in order not to have fake structures from statistical fluctuations in the Monte Carlo, we applied a smoothing function. Fig. 10 shows $A(M, P_t)$ after smoothing.

7 $\pi^+\pi^-$ cross sections

For each M, P_t bin we divide the data by the acceptance to get the corrected mass distribution, and use the effective luminosity to get the cross section $d\sigma/dM$, as shown in Figs. 11 and 12. Fig. 11 ilustrates a fact, that the resonances structure in range 1.0 1.5 GeV/c^2 is preserved. The mass spectra shows broad continuum below 1 GeV/c^2 and sharp drop at 1 GeV/c^2. Fig. 12 presents invariant mass distribution of 2 particles assuming pion masses zoomed to range 1.5 2.5 GeV/c^2. It shows an exponential drop with bumping structure.

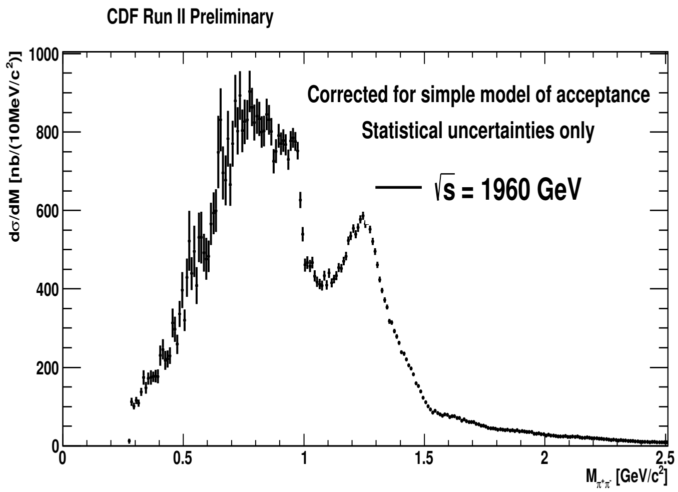

Figure 11: Invariant mass distribution of 2 particles assuming pion masses - corrected for acceptance. $\sqrt{s} = 1960$ GeV

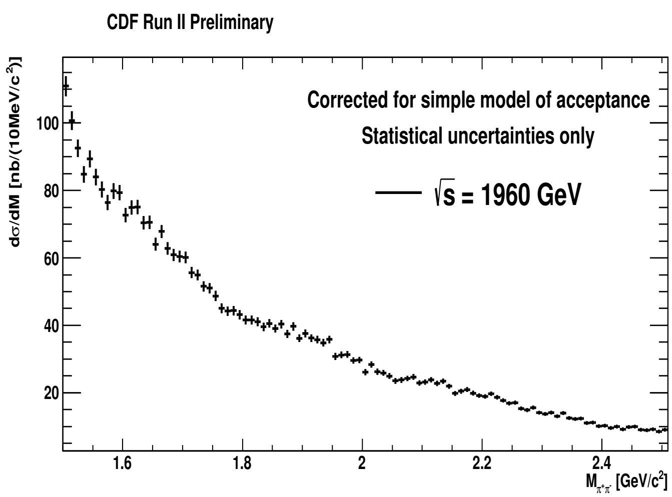

Figure 12: Invariant mass distribution of 2 particles assuming pion masses - corrected for acceptance. $\sqrt{s} = 1960$ GeV

8 Summary and Conclusions

This is a work in progress. For now (July 2012) we have shown a large sample of exclusive h^+h^- events (much larger than in other experiments), mostly $\pi^+\pi^-$, that show several resonance features. Other channels are being studied.

References

[1] Quantum Chromodynamics and the Pomeron, J.R.Forshaw and D.A.Ross, Cambridge Lecure Notes in Physics, Cambridge University Press, 1997.

[2] V.Barone and E.Predazzi, High Energy Particke Diffraction, Springer, 2002.

[3] S.Donnachie, G.Dosch, P.Landshoff and O.Nachtmann, Pomeron Physics and QCD, Cambridge University Press, 2002.

[4] M.G.Albrow, T.D.Coughlin, and J.R.Forshaw, Central exclusive particle production at hadron colliders, Prog.Part.Nucl.Phys. **65**, 149 (2010).

[5] T.Aaltonen *et al.*(CDF), Phys.Rev.Lett. **98**, 112001 (2007).

[6] T.Aaltonen *et al.* (CDF Collaboration), Phys.Rev.Lett. **102** 242001 (2009).

[7] T.Aaltonen *et al.* (CDF), Phys.Rev.Lett. **102** 222002 (2009).

[8] T.Aaltonen *et al.* (CDF), Phys.Rev.Lett. **99**, 242002 (2007); T.Aaltonen *et al.* (CDF), Phys.Rev.Lett. **108**, 081801 (2012).

[9] J.L.Rosner, Phys. Rev. D **74** 076006 (2006).

[10] T.Akesson *et al.* (AFS Collaboration, C and jets), Phys.Lett. **128B**, 354 (1983).

[11] C.Amsler, T.Gutsche, S.Spanier and N.A.Tornqvist, Note on Scalar Mesons in K.Nakamura *et al.*, (Particle Data Group), J. Phys. G. **37** 075021 (2010).

[12] P.Lebiedowicz, R. Pasechnik, A.Szczurek, Nucl.Phys.Proc.Suppl. 219-220 (2011).

[13] D.Robson, Nucl. Phys. **B 130**, 328 (1977).

[14] T.Akesson *et al.* Phys. Lett. **133B** 268 (1983); T.Akesson *et al.*, Nucl. Phys. **B 264**, 154 (1986)

[15] K.L.Au, D.Morgan and M.R.Pennington, Phys. Rev. D **35**, 1633 (1987); K.L.Au, D.Morgan and M.R.Pennington, DTP-86/8, Proc. 21st Rencontre de Moriond (1986).

[16] P.Minkowski and W.Ochs, Eur. Phys. J **C9** 283 (1999).